ENVIRONMENTAL RESEARCH
LETTERS

LETTER • OPEN ACCESS

Future changes in extreme heatwaves in terms of intensity and duration over the CORDEX-East Asia Phase Two domain using multi-GCM and multi-RCM chains

To cite this article: Young-Hyun Kim *et al* 2023 *Environ. Res. Lett.* **18** 034007

ENVIRONMENTAL RESEARCH
LETTERS

LETTER

Future changes in extreme heatwaves in terms of intensity and duration over the CORDEX-East Asia Phase Two domain using multi-GCM and multi-RCM chains

Young-Hyun Kim[1], **Joong-Bae Ahn**[1,*], **Myoung-Seok Suh**[2], **Dong-Hyun Cha**[3], **Eun-Chul Chang**[2], **Seung-Ki Min**[4], **Young-Hwa Byun**[5] and **Jin-Uk Kim**[5]

[1] Department of Atmospheric Sciences, Pusan National University, Busan, Republic of Korea
[2] Department of Atmospheric Science, Kongju National University, Gongju, Republic of Korea
[3] School of Urban and Environmental Engineering, Ulsan National Institute of Science and Technology, Ulsan, Republic of Korea
[4] Division of Environmental Science and Engineering, Pohang University of Science and Technology, Pohang, Republic of Korea
[5] Climate Change Research Team, National Institute of Meteorological Sciences, Jeju, Republic of Korea
[*] Author to whom any correspondence should be addressed.

E-mail: jbahn@pusan.ac.kr

Keywords: heatwaves, multi-GCM and multi-RCM chains, representative concentration pathways (RCPs), shared socioeconomic pathways (SSPs), CMIP5, CMIP6, CORDEX-east Asia phase 2

Supplementary material for this article is available online

OPEN ACCESS

RECEIVED
20 July 2022

REVISED
23 November 2022

ACCEPTED FOR PUBLICATION
30 January 2023

PUBLISHED
14 February 2023

Abstract

An extreme heatwave, in terms of intensity and duration, is projected to occur at the end of the 21st century (2071–2100) over the whole of East Asia. The projection is calculated using daily maximum temperature data of 25 km horizontal resolution produced by 12 general circulation model-regional climate model chains participating in the CORDEX-East Asia Phase 2 project. An 'extreme' heatwave is defined as one in which the heatwave magnitude (HWM), which is the accumulated daily intensity of a heatwave during the heatwave period, is higher than the 95th percentile of the HWM for the reference period (1981–2005). In historical simulations, heatwaves have occurred mainly from April to June in India, in April and May in Indochina, from June to August in China and Mongolia, and in July and August in the Korean Peninsula and Japan; most heatwaves last three to four days. In India and Indochina, long-lasting and intense heatwaves occur more often than in other regions. In future, heatwave intensity will increase, the average duration of heatwaves will be approximately two to three weeks, and the heatwave season will be lengthened. Therefore, extreme heatwaves will occur more frequently and strongly. Under two representative concentration pathway scenarios (RCP2.6 and RCP8.5) and two shared socioeconomic pathway scenarios (SSP1-2.6 and SSP5-8.5), the proportion of extreme heatwaves to all heatwave events will increase from 5.0% (historical) to 8.0%, 20.8%, 19.3%, and 36.3%, and the HWM of the extreme heatwave will be 1.4, 3.5, 3.0, and 9.0 times stronger, respectively. The main reason for the increase in the HWM of extreme heatwaves is the increased duration rather than the daily intensity of the heatwaves. In East Asia, the temporal and regional disparities of heatwave damage will be much more prominent as extreme heatwaves become stronger and more frequent in these regions and during the periods that are more affected by heatwaves in the present day.

1. Introduction

The frequency and intensity of heatwaves have been increasing worldwide due to the acceleration of global warming (Meehl and Tebaldi 2004, Zhao *et al* 2019, Perkins-Kirkpatrick and Lewis 2020, IPCC 2021). In East Asia, one of the regions vulnerable to climate change, unprecedented heatwaves have occurred in recent years. For instance, the highest daily maximum temperature since observations commenced was recorded in many parts of East Asia, including South Korea and Japan, when record-breaking

heatwaves occurred in 2018 (KMA 2019, WMO 2019). In India, a heatwave that ranked among the deadliest global events occurred in 2015, the average number of heatwave days rose by 82.6% year-on-year in 2019, and the average daily maximum temperature in March was the highest in the 121 years since meteorological observations began, as heatwaves occurred early in 2022. In Hanoi, the highest temperature in 100 years was recorded due to heatwaves in 2019, and the longest heatwave since 1971 hit northern Vietnam in 2020.

It is expected that human, social, and economic damage caused by heatwaves will be more severe, because not only are the frequency and intensity of heatwaves increasing but the timing of heatwaves is also diversifying. In order to mitigate and prepare for damage caused by heatwaves, it is essential to identify regions and time periods that are relatively more vulnerable to heatwaves, and to project changes in extreme heatwaves with high intensity and long duration. Based on climate modeling, many studies have demonstrated increases in heatwaves over East Asia under the green house gas emissions scenarios (Gu *et al* 2012, Im *et al* 2017, 2019, Mishra *et al* 2017, Li *et al* 2019, Rohini *et al* 2019, Su and Dong 2019, Wang *et al* 2019, Dong *et al* 2021, Xie *et al* 2021). These studies had limitations in quantitatively comparing the characteristics of heatwaves in each region of East Asia because they analyzed heatwaves only for a specific country by applying different thresholds. Recently, several studies investigated future changes in heatwaves on a global scale (Perkins-Kirkpatrick and Gibson 2017, Dosio *et al* 2018, Baldwin *et al* 2019, Zhao *et al* 2019). However, some of those studies used only the general circulation model (GCM) data that have a coarse spatial resolution, so they were limited when simulating detailed features of extreme events on a regional scale. Several studies used fine-scale climate projections dynamically or statistically downscaled from GCM results, but offered limited reliability in future climate projections because they were produced from a single GCM. In addition, most of the aforementioned studies mainly focused on changes in the annual average or annual accumulated values of characteristic heatwaves.

The objective of this study is to investigate future changes in extreme heatwaves with a long duration and a strong intensity over the whole of East Asia at the end of the 21st century by applying a heatwave threshold considering spatiotemporal climate conditions. Many studies demonstrated the added value of the regional climate model (RCM) compared to the GCM in simulating extreme events (Giorgi *et al* 2014, Torma *et al* 2015, Ahn *et al* 2016, Park *et al* 2020, Ciarlo *et al*, 2021). In this regard, a multi-model ensemble of daily maximum temperature (Tmax) data of 25 km horizontal resolution, downscaled by 12 GCM-RCM chains, consisting of combinations of four GCMs and five RCMs, is used.

2. Data and analysis method

2.1. Model and observation data

In order to project extreme heatwaves over the whole of East Asia at the end of the 21st century, Tmax data of 25 km horizontal resolution produced by 12 GCM-RCM chains participating in the Coordinated Regional Climate Downscaling Experiment-East Asia Phase 2 (CORDEX-EA2) (http://cordex-ea.climate.go.kr/) international cooperation project, which was established by the World Climate Research Programme (WCRP) are used (figure S1). We utilize global projections simulated by GCMs from CMIP5 forced by representative concentration pathway scenarios (RCP2.6 and RCP8.5) and from CMIP6 forced by shared socioeconomic pathway scenarios (SSP1-2.6 and SSP5-8.5). The configurations of the 12 GCM-RCM chains are summarized in table 1. The multi-model ensemble (ENS), which is the average of GCM-RCM chains with equal weighting, is mainly used to enhance the reliability of future projections of Tmax. The average of HG2_CCLM, HG2_RegCM, HG2_MM5, MPI_WRF, MPI_CCLM, MPI_MM5, GFDL_WRF, and GFDL_RegCM (UKESM_WRF, UKESM_CCLM, UKESM_GRIMs, and UKESM_RegCM) for historical, RCP2.6, and RCP8.5 (historical, SSP1-2.6 and SSP5-8.5) simulations are denoted ENS_CMIP5_HIS, ENS_RCP26, and ENS_RCP85 (ENS_CMIP6_HIS, ENS_SSP126, and ENS_SSP585), respectively. The average of 12 GCM-RCM chains for historical simulation is denoted ENS_ALL_HIS.

Analysis is conducted over the whole CORDEX-EA2 domain, as shown in figure 1. In order to analyze the characteristics of heatwaves in each region in East Asia with their various climate zones, the whole domain is divided into eight subdomains: the Korean Peninsula (R1, 33–42° N, 125–130° E), East China (R2, 23–42° N, 104–123° E), West China (R3, 31–42° N, 80–104° E), India (R4, 8–27° N, 74–84° E), Mongolia (R5, 42–52° N, 88–120° E), Japan (R6, 30–42° N, 130–145° E and 42–45° N,140–145° E), Indochina (R7, 8–23° N,92–110° E), and Northeast China (R8, 42–54° N,120–135° E). Ocean grid values are masked as missing values. The Tmax, which is a variable used to define a heatwave, is calculated as the highest value among the three-hourly temperature data, and then is bias-corrected using a variance scaling (a method to correct both mean and variance of a variable) to reduce systematic bias in each model (Teutschbein and Seibert 2012) (see SI). The analysis period is 25 years for the historical simulation (1981–2005) and 30 years for RCP or SSP simulations (2071–2100). While heatwaves occur in July and August in most regions of East Asia including the Korean Peninsula, China, Mongolia, and Japan (Yeo *et al* 2019; Gao *et al* 2018; Piver *et al* 1999; Yuan *et al* 2016), they occur from April to June in India and Indochina

Table 1. Twelve GCM-RCM chains and the configurations used in this study.

GCM-RCM Chains	HG2_CCLM	HG2_RegCM	HG2_MM5	MPI_WRF	MPI_CCLM	MPI_MM5	GFDL_WRF	GFDL_RegCM	UKESM_WRF	UKESM_CCLM	UKESM_GRIMs	UKESM_RegCM
	Coupled Model Intercomparison Project phase5 (CMIP5)						CMIP5		Coupled Model Intercomparison Project phase6 (CMIP6)			
GCM	HadGEM2-AO			MPI-ESM-LR			GFDL-ESM2M		UK-ESM			
RCM	CCLM	RegCM	SNU-MM5	WRF	CCLM	SNU-MM5	WRF	RegCM	WRF	CCLM	GRIMs	RegCM
Forcing Scenarios	Representative Concentration Pathways			Representative Concentration Pathways (RCP2.6 and RCP8.5)					Shared Socioeconomic Pathways (SSP1-2.6 and SSP5-8.5)			
Long/Short waves	Ritter and Geleyn	NCAR CCM3	CCM2 package	CAM	Ritter and Geleyn	CCM2 package	CAM	NCAR CCM3	CAM	Ritter and Geleyn	Chou *et al*, 1999/Chou and Suarez, 1999	NCAR CCM3
Explicit moisture scheme	Extended DM	SUBEX	Reisner2	WSM3	Extended DM	Reisner2	WSM3	SUBEX	WSM3	Extended DM	—	SUBEX
Land Surface	TERRA-ML	NCAR CLM3.5	NCAR CLM3/ NOAH LSM	Noah	TERRA-ML	NCAR CLM3/ NOAH LSM	NOAH LSM	NCAR CLM3.5	NOAH LSM	TERRA-ML	NOAH LSM	NCAR CLM4.5
PBL	Davis and Turner	Holtslag	YSU	YSU	Davis and Turner	YSU	YSU	Holtslag	YSU	Davis and Turner	YSU	Holtslag
Cumulus	Tiedtke-mass-flux-convection	MIT-Emanuel	Kain-Fritch	Bats-Miller	Tiedtke-mass-flux-convection	Kain-Fritch	Bats-Miller-Janjic	MIT-Emanuel	Bats-Miller-Janjic	Tiedtke-mass-flux-convection	Simplified Arakawa-Schubert	MIT-Emanuel
lat × lon	251×396	251×396	260×405	250×395	251×396	260×405	250×395	251×396	250×395	251×396	252×401	251×396

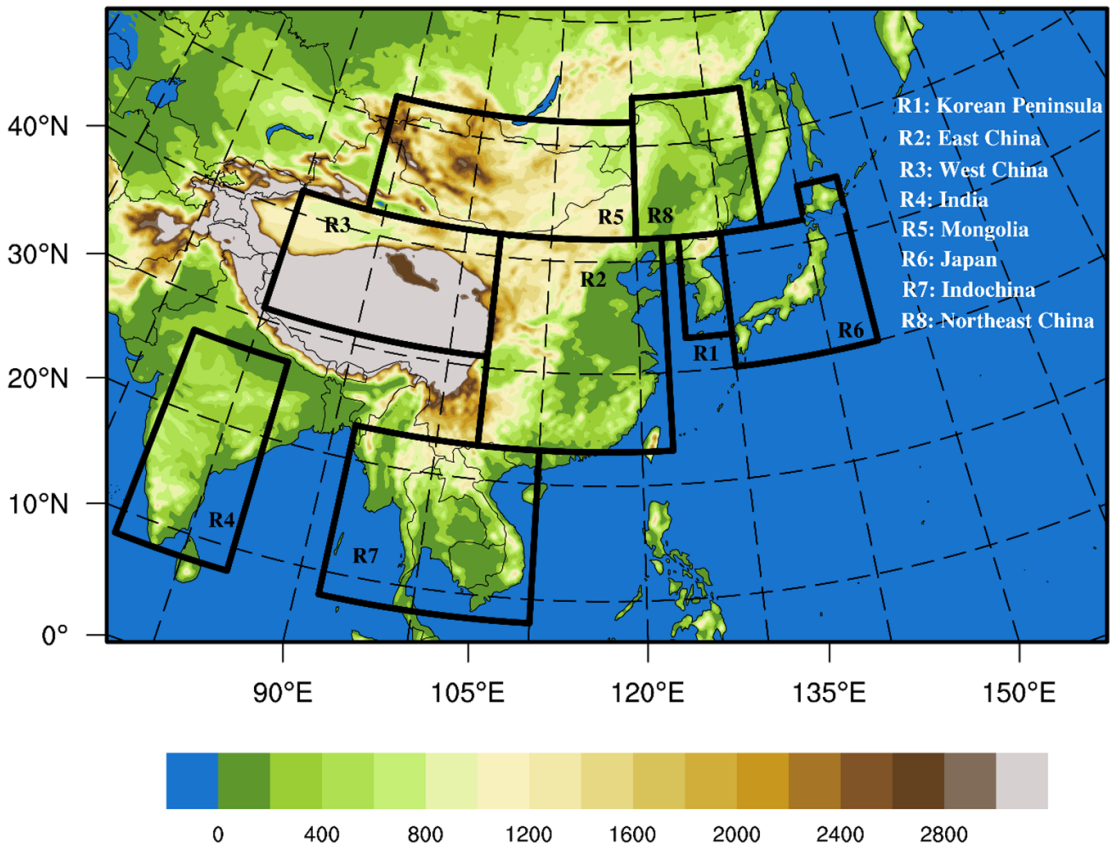

Figure 1. CORDEX-East Asia Phase 2 domain and topography (unit: m). Boxed areas indicate the eight subdomains (R1-R8).

(Thawillarp *et al* 2015, Mishra *et al* 2017, Thirumalai *et al* 2017, Kumar and Mishara 2019, Rachutorn *et al* 2019). Therefore, the heatwave occurrence period in East Asia selected is from April 1 to September.

ERA5 reanalysis data provided by the European Center for Medium-Range Weather Forecasts is used for model evaluation and bias correction. For this, gridded Tmax data simulated by GCM-RCM chains are interpolated into the ERA5 grid (0.25° × 0.25°) by using simple inverse distance weighting.

2.2. Definition of a heatwave

It is difficult to compare characteristics of heatwaves in each region of East Asia when the heatwave threshold is applied as an absolute value for an entire region with different climate conditions. For example, when people are exposed to the same temperature, the people who live in a warm climate feel thermally comfortable, whereas people who live in a cold climate feel thermally uncomfortable. Therefore, a heatwave threshold considered for regional and temporal climate conditions is applied in this study. The daily heatwave threshold is defined as the 90th percentile of Tmax within a 31-day window centered on each Julian day (i.e. 15 days before and after the day) for the reference period (Russo *et al* 2015). A heatwave is defined as a period where the Tmax is above the heatwave threshold for three or more consecutive days.

The characteristics of a heatwave are estimated using the method of Russo *et al* (2015). The heatwave magnitude (HWM) is defined as the sum of the daily intensities of the heatwave within a heatwave period, where the daily intensity of heatwave (HWId) is calculated as follows:

$$\mathrm{HWId} = \begin{cases} \frac{T_d - T_{25y25p}}{T_{25y75p} - T_{25y25p}} & (T_d > T_{25y25p}) \\ 0 & (T_d \leqslant T_{25y25p}) \end{cases}. \quad (1)$$

In equation (1), T_d is the Tmax on day d when the heatwave occurs, T_{25y25p} and T_{25y75p} denoting the 25th and 75th percentiles, respectively, of the annual maximum temperature during the reference period. In other words, HWId indicates the temperature anomaly on day d with respect to T_{25y25p}, normalized by the climatological interquartile range ($T_{25y75p} - T_{25y25p}$). Therefore, the daily intensity of heatwave can be compared across locations with different climate conditions. If HWId = 3, it means that the temperature anomaly on a day when a heatwave occurs with respect to the T_{25y25p} is three times the IQR.

HWM has the advantage of considering both the daily intensity and the duration of the heatwave. Hence, an extreme heatwave in terms of duration and intensity is defined as a heatwave in which HWM is

higher than the 95th percentile of the HWM for the reference period and referred as HWM95p heatwave.

3. Results

3.1. Evaluation of present-day simulated daily maximum temperatures

In order to quantitatively evaluate the performance of models in simulating Tmax for the reference period, a Taylor diagram is presented in figure S2. The spatial correlation coefficients between ENS_ALL_HIS and ERA5 (SCC) and the temporal standard deviations of ENS_ALL_HIS, normalized by that of ERA5 (NSD) for Tmax before bias correction (Tmax_ORG) ranges from 0.82 to 0.98 and from 0.82 to 1.05 in the eight subdomains. In general, the simulated Tmax in ENS_ALL_HIS are similar to ERA5 in East Asia. The SCC for corrected Tmax via the variance-scaling method (Tmax_VS) ranges from 0.97 to 1.00, and the NSD for Tmax_VS is close to 1.0 in the eight subdomains. The distribution range and shape of the probability distribution functions for Tmax_VS is more similar than Tmax_ORG to those of ERA5 (figure S3). These mean that the bias correction improve the spatial variance and the correlation of Tmax. Therefore, a heatwave is analyzed by using the bias-corrected Tmax from the variance-scaling method.

In all of East Asia, which has various climate types, not only the range of Tmax but also the timing of the annual maximum temperatures vary by region. Figure S4 shows the spatial distributions of Julian days with the highest five-day moving average Tmax (hereafter, 5D_Tmax). In ERA5 (figure S4(a)), 5D_Tmax is the highest in July or August in most regions of East Asia including the Korean Peninsula, China, Mongolia, and Japan, whereas it is the highest in April or May for India and Indochina (Bangladesh, Cambodia, Laos, Myanmar, Thailand, and Vietnam). The month with the highest 5D_Tmax in eight subregions derived from twelve GCM-RCM chains, is also similar to that derived from ERA5 (figure S5). These results show that the timing of the annual maximum temperature is captured in historical simulations quite well.

To investigate the characteristics of Tmax during the period when heatwaves mainly occur in each region of East Asia, the average Tmax for a total of 61 d, before and after 30 d from the Julian day with the highest 5D_Tmax (Tmax_HP), at each grid point are shown in figure 2. In ERA5 (figure 2(a)), the Tmax_HP is relatively high in India and Indochina, although it is relatively low in West China, where the Tibetan Plateau is located, compared to other regions. Those climatological characteristics of Tmax_HP according to latitude, longitude, and terrain features are simulated quite well in ENS_ALL_HIS (figures 2(b) and (g)). Figure S6 shows that bias for Tmax_HP over East Asia derived from twelve GCM-RCM chains, ENS_CMIP5_HIS, ENS_CMIP6_HIS, and ENS_ALL_HIS compared with ERA5. Although those tend to underestimate Tmax_HP, the magnitude of biases are not large. All ensemble results show better performance in the daily maximum temperature than each GCM-RCM chain. The bias derived from ENS_CMIP6_HIS is larger than that derived from ENS_CMIP5, which might be because ENS_CMIP6_HIS is forced by only one GCM, while ENS_CMIP5_HIS is forced by three GCMs. Figure S7 shows that the magnitude of difference for Tmax_HP derived from ENS_CMIP5_HIS or ENS_CMIP6_HIS and that derived from ENS_ALL HIS are neither large. Therefore, the analysis results for the present climate show only ENS_ALL_HIS, even though a future change is calculated based on the differences between ENS_RCP26 or ENS_RCP85 (ENS_SSP126 or ENS_SSP585) and ENS_CMIP5_HIS (ENS_CMIP6_HIS).

3.2. Evaluation of simulated present-day heatwave intensity and duration

The heatwave threshold is relatively high in July or August on the Korean Peninsula, in China, in Mongolia, and in Japan, as well as in May for India and in April for Indochina (figures S8(b)–(g)). These months coincide with the month of the highest 5D_Tmax derived from ENS_ALL_HIS (figure S4(b)). The heatwave threshold is higher in India and Indochina but lower in West China, than in other regions (figure S8(a)), which is similar to the spatial distribution of Tmax_HP derived from ENS_ALL_HIS (figure 2(b)). Therefore, the heatwave threshold spatiotemporally captures the climatological features of Tmax quite well.

Prior to future projections of extreme heatwaves, the models performance on heatwave intensity and duration for the historical period is examined. Figures 3 and 4 show the spatial distributions for climatology of the accumulated daily intensity of heatwave and the heatwave frequency at various durations, as well as bias derived from ERA5 and ENS_ALL_HIS. In ERA5, heatwave intensity is relatively high in some parts of China, India, and Indochina, compared to other regions. Heatwave intensity is highest in July or August on the Korean Peninsula, in China, in Mongolia, and in Japan, as well as in May for India and in April for Indochina. These periods coincide with periods when the Tmax is the highest (figure S4(a)). The frequency of heatwaves is higher in East China and Indochina than in other regions, and most heatwaves last three to four days over the whole of East Asia. In India and Indochina, heatwaves that last more than eight days occur, which is rare in other regions. In ENS_ALL_HIS, the heatwaves intensity and the frequency of heatwaves at various durations is overestimated in most regions of East Asia, including some parts of China, India, and Indochina. Nevertheless, spatial distribution of monthly accumulated intensities of heatwaves and the frequency of heatwaves of

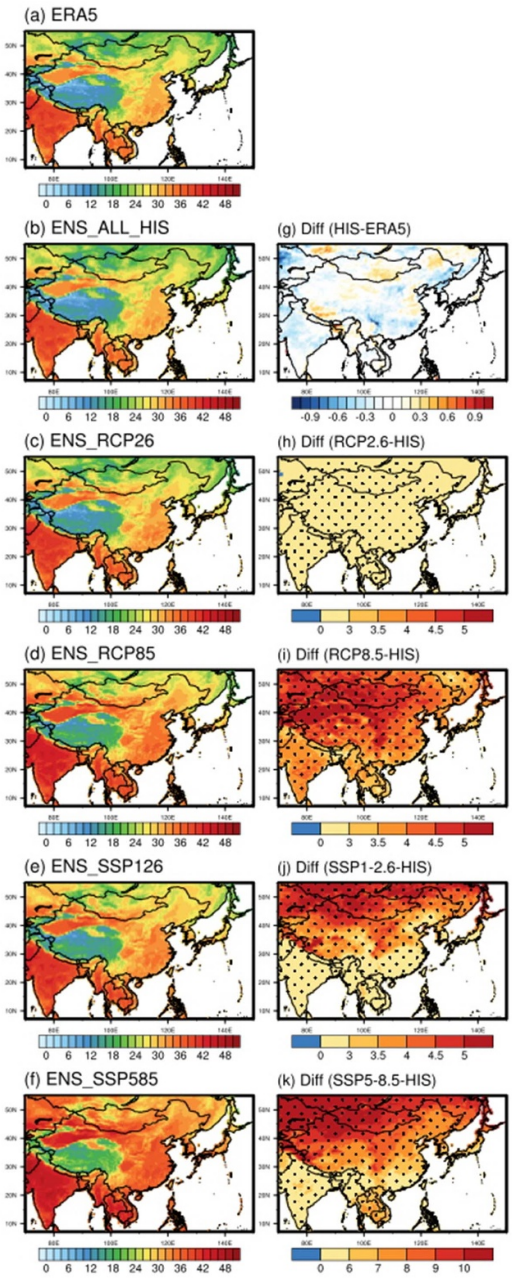

Figure 2. Spatial distributions of average daily maximum temperatures for a total of 61 days, before and after 30 days from the Julian day with the highest 5 days moving average daily maximum temperature (Tmax_HP) derived from (a) ERA5, (b) ENS_ALL_HIS, (c) ENS_RCP26, (d) ENS_ RCP85, (e) ENS_SSP126, and (f) ENS_SSP585. Bottom panels show (g) the bias of ENS_ALL_HIS compared with ERA5, and future changes in Tmax_HP under (h) RCP2.6, (i) RCP8.5, (j) SSP1-2.6, and (k) SSP5-8.5 scenarios (unit: °C). The grid points with black dots denote the 95% confidence level based on a Student's *t*-test.

various durations are similar to those in ERA5. This means ENS_ALL_HIS captures the intensity and duration of heatwaves in East Asia in the present day climate quite well.

3.3. Changes in daily maximum temperature

The delay in the Julian day with the highest Tmax means that the length of the boreal summer will be longer after the northern hemisphere's summer solstice. In all scenarios, the Julian day with the highest 5D_Tmax is delayed in some parts of East Asia (figures S4(h)–(k)). Therefore, the month with the highest 5D_Tmax changes to August from July on the Korean Peninsula in the SSP1-2.6 scenario (figure S4(e)), and that changes to August from July on the Korean Peninsula and in some parts of West China and Mongolia, but changes to May from April for Vietnam and Thailand in Indochina in SSP5-8.5 scenario (figure S4(f)).

In all scenarios, Tmax_HP increases over the whole of East Asia, particularly in the high-latitude regions than in India and Indochina, which already experience extreme temperatures in Historical simulation (figures 2(h)–(k)). The area-averaged Tmax_HP for East Asia increased from 26.2 °C (Historical) to 27.4 °C (RCP2.6), 30.2 °C (RCP8.5),

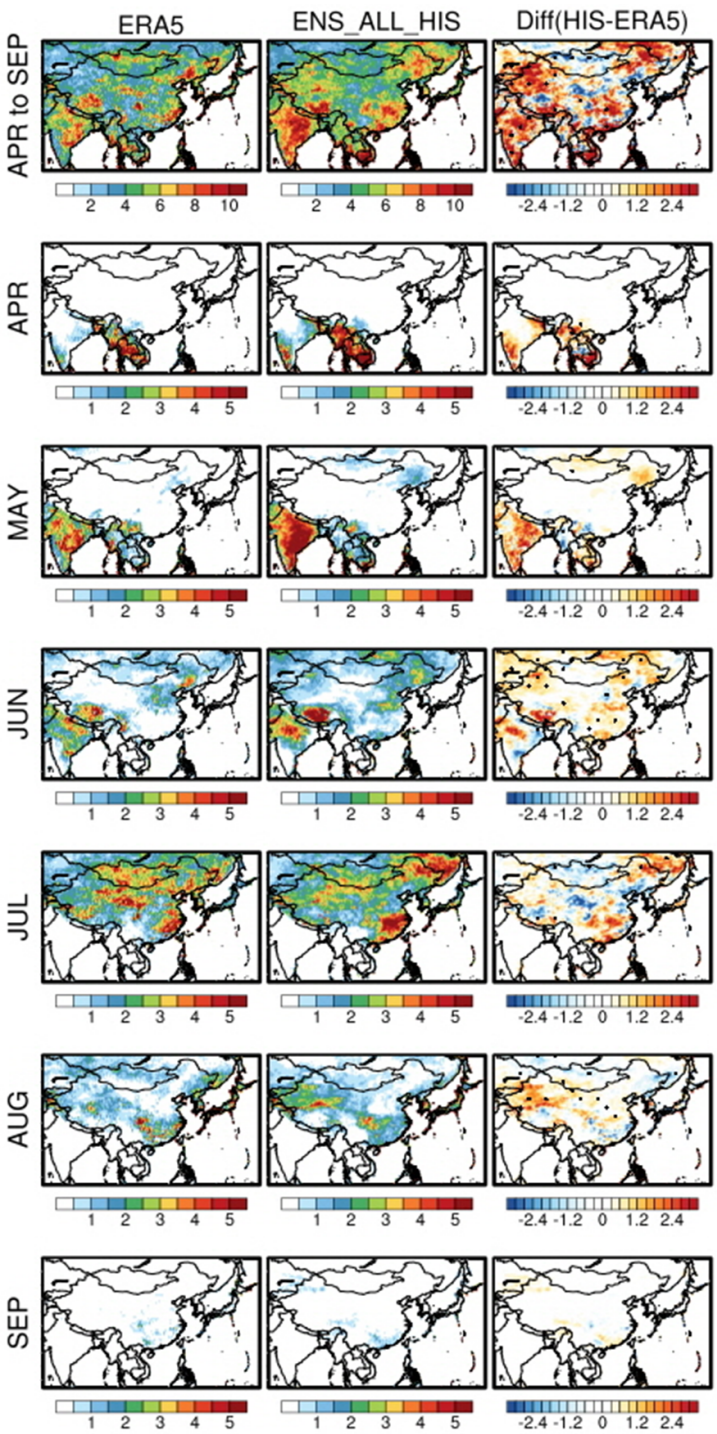

Figure 3. Spatial distributions of the climatology of the accumulated daily intensity of heatwave derived from ENS_ALL_HIS. The grid points with black dots denote the 95% confidence level based on a Student's *t*-test.

29.4 °C (SSP1-2.6), and 33.6 °C (SSP5-8.5), respectively, which means that Tmax_HP increase more in the high emissions scenario.

3.4. Changes in extreme heatwave in terms of intensity and duration

In this section, we analyze the future changes in extreme heatwave in terms of intensity and duration, as the Tmax increases over a 30 year period (2071–2100). Figures 5 and S9 show the future changes in the accumulated daily intensity of heatwave. In all scenarios, the heatwave intensity increases over the whole of East Asia, especially in India and Indochina, where the heatwave intensity is already high in the present-day and in some parts of East and West China. In the SSP5-8.5 scenario, the heatwave intensity is also high in West Mongolia. In all scenarios, the heatwaves intensity is highest in the same months as in the Historical simulation because the intensity increases even more in the months when it is already

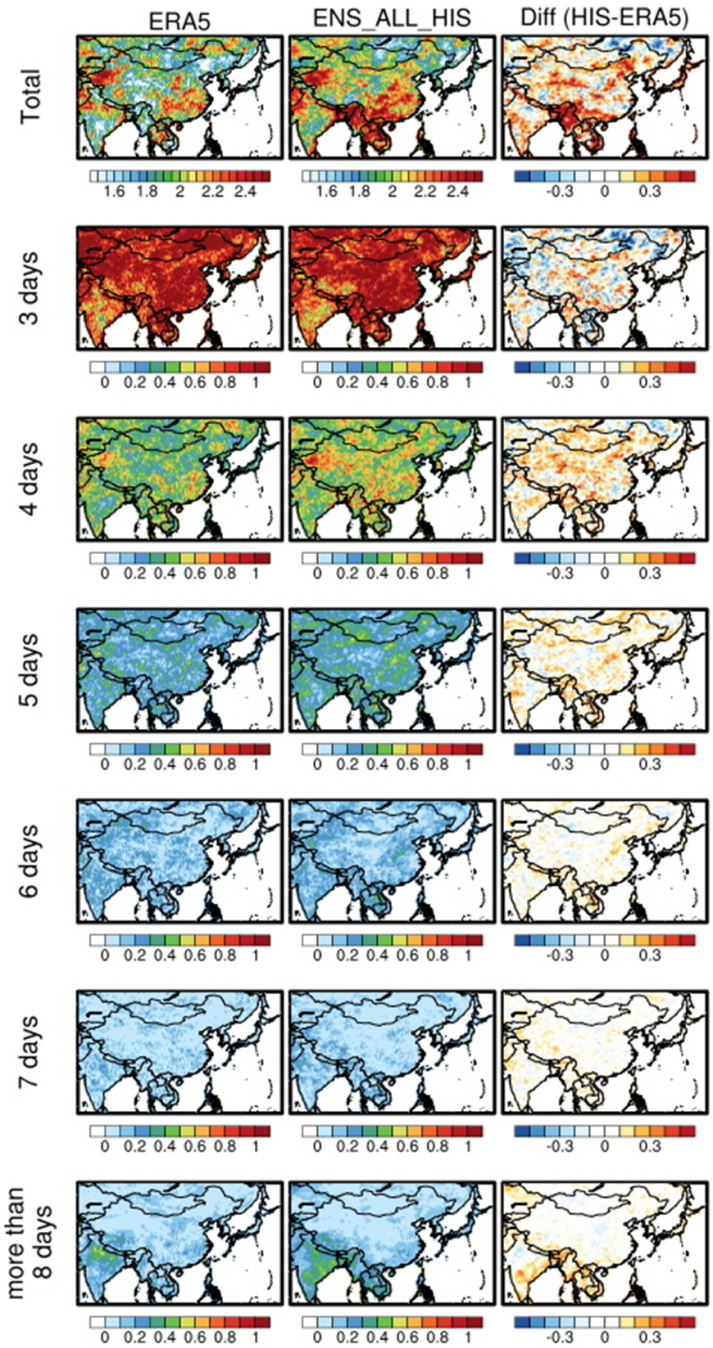

Figure 4. Spatial distributions of the climatology of the heatwave frequency at various durations derived from ENS_ALL_HIS (unit: events).

high in the Historical simulation (in July or August for the Korean Peninsula, China, Mongolia, and Japan; in May for India; in April for Indochina). Therefore, the regional and temporal differences in the intensity of heatwaves will become larger.

In addition, the heatwave intensity increases even when heatwaves do not occur in the historical simulation: in June or September on the Korean Peninsula; May and September for East China; May or September for West China; June for South India; September for Japan; June or July for Indochina under the RCP8.5 and SSP1-2.6 scenarios; May, June, and September on the Korean Peninsula; April, May, and September for East China; May and September for West China; from June to September for South India and Indochina; April and September for Mongolia; June and September for Japan; September for Northeast China under the SSP5-8.5 scenario.

Longer lasting heatwaves may contribute to increased risks from heatwaves due to prolonged exposure. Figure 6 presents the climatology of the heatwave frequency for various durations in East Asia and the eight subdomains. In the RCP2.6 scenario, the shorter the duration, the higher the frequency of heatwaves over the whole of East Asia. In the RCP8.5 and SSP1-2.6 scenarios, the shorter the duration, the

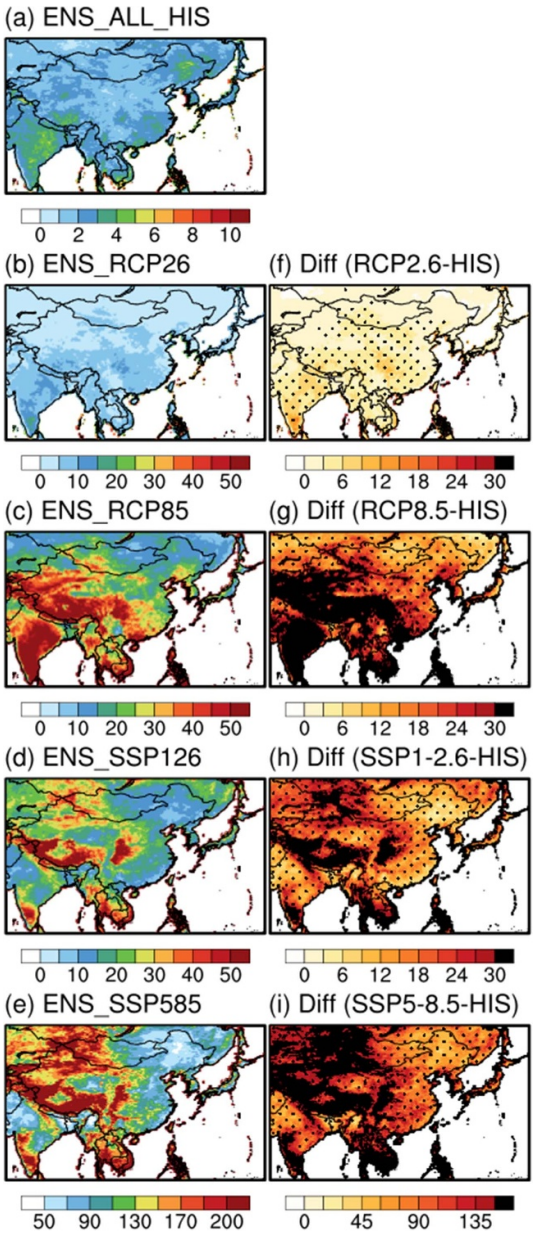

Figure 5. Spatial distributions of the accumulated daily intensity of heatwaves during the heatwave period derived from (a) ENS_ALL_HIS, (b) ENS_RCP26, (c) ENS_ RCP85, (d) ENS_SSP126, and (e) ENS_SSP585. Right panels show the future changes in the accumulated daily intensity of heatwaves under (f) RCP2.6, (g) RCP8.5, (h) SSP1-2.6 and (i) SSP5-8.5 scenarios. The grid points with black dots denote the 95% confidence level based on a Student's *t*-test.

higher the frequency of heatwaves in most regions, except for India and Indochina, where the frequency of heatwaves lasting more than 10 days is the highest or as high as the frequency of heatwaves lasting three or four days. In the SSP5-8.5 scenario, most heatwaves last more than 10 days over the whole of East Asia. In addition, heatwaves lasting more than 20 days, which do not occur everywhere in East Asia in the Historical simulation, occur in India and Indochina under the RCP2.6 scenario and in all of East Asia under other scenarios.

As long-lasting heatwaves will occur more often, the average duration of a heatwave in East Asia increases from 4.3 days (Historical) to 5.2 days (RCP2.6), 12.7 days (RCP8.5), 9.9 days (SSP1-2.6), and 22.4 days (SSP5-8.5). In India and Indochina, the average duration of heatwaves is around two to three weeks under the RCP8.5 and SSP1-2.6 scenarios, and one month under the SSP5-8.5 scenario, which are much longer than in other regions.

Finally, we investigate the future changes in extreme heatwaves, as their daily intensity increases and the durations lengthen (figure 7). The threshold of HWM95p heatwaves is high in some parts of China, India, and Indochina, where the heatwave intensity is high in the Historical simulation (figure 3). In the historical simulation, the proportion of HWM95p heatwave to the total number of heatwaves is similar in all of East Asia, while the mean HWM of HWM95p heatwaves is higher in

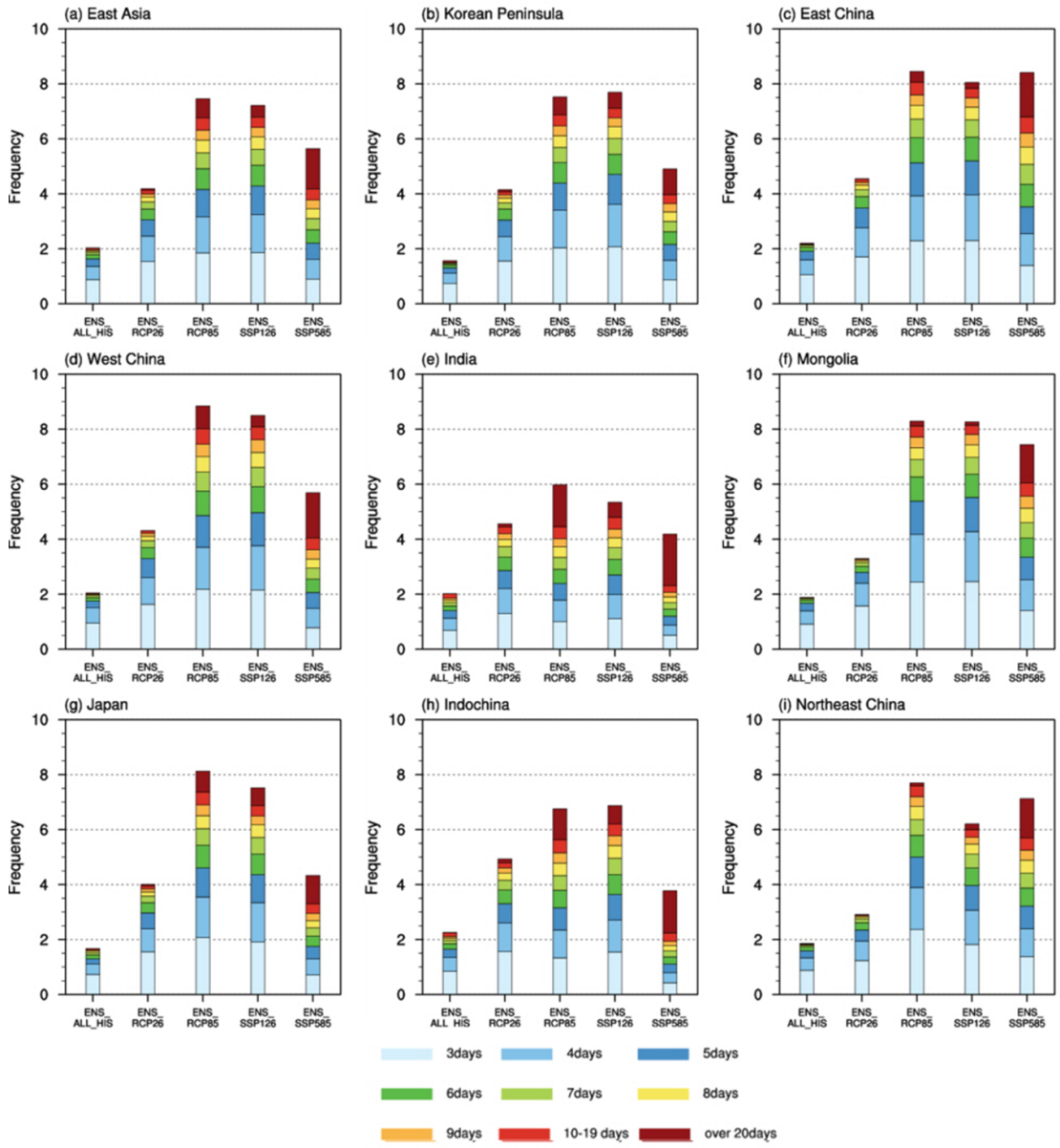

Figure 6. Climatology of heatwave frequency at various durations over (a) East Asia, (b) the Korean Peninsula, (c) East China, (d) West China, (e) India, (f) Mongolia, (g) Japan, (h) Indochina and (i) Northeast China (unit: events).

India and Indochina than in other regions. In all scenarios, the proportion and mean HWM of the HWM95p heatwave increase over the whole of East Asia and increase more in East and West China, India, and Indochina than in the other regions. Therefore, the regional difference of the proportion and mean HWM of HWM95p heatwave become large. The area-averaged the proportion of HWM95p heatwave in East Asia increase from 5.0% (historical) to 8.0% (RCP2.6), 20.8% (RCP8.5), 19.3% (SSP1-2.6), and 36.3% (SSP5-8.5), respectively. The mean HWM of the HWM95p heatwave is 1.4 times (RCP2.6), 3.5 times (RCP8.5), 3.0 times (SSP1-2.6), 9.0 times (SSP5-8.5) more intense than the historical simulation. In other words, extreme heatwaves occur much more frequently and intensely in East Asia, especially the regions more affected by extreme heatwaves in the present day.

The reasons for the increase in HWM of extreme heatwaves are increases in daily intensity or duration (or both daily intensity and duration) of the heatwave. In order to analyze the impact of daily intensity and duration of heatwaves on increases in HWM of extreme heatwaves, scatter plots for HWM95p heatwave duration (HWD_HWM95p) and averages for the daily intensity within the HWM95p heatwave period (HWI_HMW95p) in the eight subdomains are presented in figure 8. The mean for HWI_HWM95p derived from ENS_ALL_HIS (Mean_HWI) is relatively high on the Korean Peninsula, in India, and in Northeast China, and the maximum HWI_HWM95p (Max_HWI) is relatively

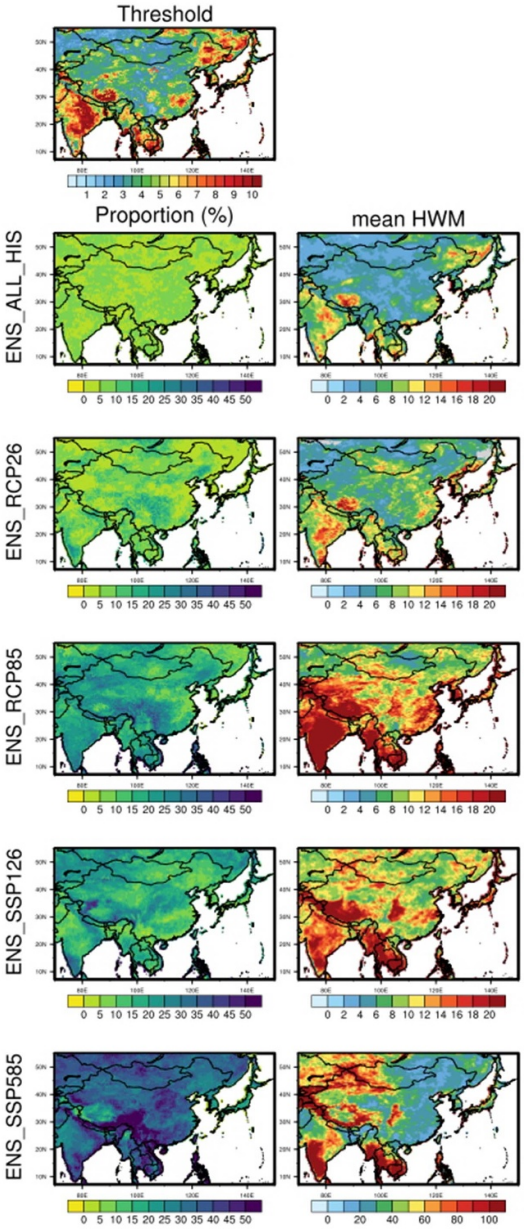

Figure 7. Spatial distributions of the threshold of HMW95p heatwave, the proportion of HWM95p heatwaves to the total number of heatwaves (unit: %), and the mean HWM of HWM95p heatwave derived from ENS_ALL_HIS, ENS_RCP26, ENS_RCP85, ENS_SSP126, and ENS_SSP585.

high for India, Indochina, East China, and Northeast China. Both the mean for HWI_HWM95p derived from ENS_ALL_HIS (Mean_HWD) and the maximum HWD_HWM95p (Max_HWD) are relatively long in India and Indochina.

If HWI_HWM95p is higher (lower) than Mean_HWI, and if HWD_HWM95p is shorter (longer) than Mean_HWD, the increase in the daily intensity (duration) of heatwaves has a greater impact on increases in HWM of HWM95p heatwaves than increases in the duration (daily intensity) of a heatwave. If HWI_HWM95p is higher than Mean_HWI, and HWD_HWM95p is longer than Mean_HWD, the increase in both daily intensity and duration of a heatwave has a greater impact on the increase in HWM of HWM95p heatwaves. In all scenarios, the main reason for the increase in the HWM of HWM95p heatwaves is an increase in HWD_HWM95p rather than HWI_HWM95p, except where both HWI_HWM95p and HWD_HWM95p increase over the whole of East Asia (table S1). Additionally, in ENS_RCP85, ENS_SSP126, and ENS_SSP585, HWM95p heatwaves in which HWI is higher than Max_HWI and in which HWD is longer than Max_HWD occurs over the whole of East Asia and even more occur in India and Indochina (ENS_RCP85 and ENS_SSP126) or in East and West China, India, Mongolia, and Indochina (ENS_SSP585) than in other regions. Since the HWM of such heatwaves is larger than the maximum

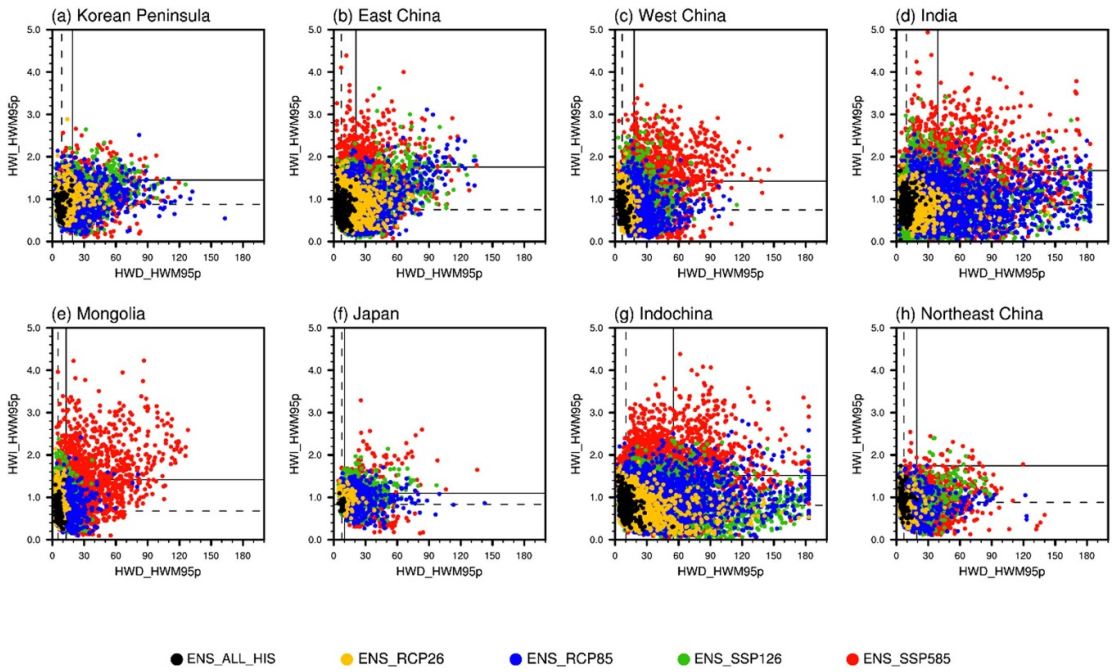

Figure 8. Scatter plots for HWM95p heatwave duration (HWD_HWM95p) and the average of daily intensity of heatwave within a HWM95p heatwave period (HWI_HWM95p) over (a) the Korean Peninsula, (b) East China, (c) West China, (d) India, (e) Mongolia, (f) Japan, (g) Indochina and (h) Northeast China. Black, yellow, blue, green, and red dots, respectively, denote HWM95p heatwaves derived from ENS_ALL_HIS, ENS_RCP26, ENS_RCP85, ENS_SSP126, and ENS_SSP585 occuring during the analysis period (25 years or 30 years). Black solid and dotted lines denote maximum and mean HWD_HWM95p and HWI_HWM95p, respectively, derived from ENS_ALL_HIS.

HWM derived from ENS_ALL_HIS, such extreme heatwaves have never occurred in the present climate.

4. Conclusions

Unprecedented heatwaves, that have occurred in various parts of East Asia in recent years, are expected to occur more frequently, with both frequency and intensity increasing due to global warming. Our study projects extreme heatwaves in terms of intensity and duration under RCP2.6, RCP8.5, SSP1-2.6 and SSP5-8.5 scenarios at the end of the 21st century, over the whole of East Asia, using Tmax data produced by 12 GCM-RCM chains.

To compare the characteristics of heatwaves in East Asia where climate types vary, a heatwave threshold considering spatiotemporal climate conditions is applied. The GCM-RCM chain reasonably simulates the characteristics of heatwaves in the present day. The duration of most heatwaves is three to four days, and the heatwave intensity is the highest in May for India, in April for Indochina, and in July or August for most other regions of East Asia, including the Korean Peninsula, China, Mongolia, and Japan. In India and Indochina, long and intense heatwaves occur more often than in other regions.

In the future, heatwaves will last, on average, two to three weeks. The heatwave intensity will increase, and the heatwave season will be longer over all of East Asia. Therefore, extreme heatwaves will occur much more frequently and intensely than in the present day. It seems that the increase in the duration of heatwaves has a greater impact on the increase in the magnitude of extreme heatwaves than an increase in the daily intensity of heatwaves. The increase in the frequency and magnitude of extreme heatwaves will be even higher in Indochina and India, which already experience extreme temperatures, and some parts of China, than in other regions.

In East Asia at the end of the 21st century, the temporal and regional disparities of heatwave damage will be much more prominent, as extreme heatwaves become stronger and more frequent in the regions and during the periods that are more affected by heatwaves in the present climate. Additionally, the occurrence timing of extreme heatwaves is expected to diversify. Future heatwaves will be exacerbated in urban regions considering the urban heat island effect, which could not be taken into account because the data has a resolution limitation.

Data availability statement

The data that support the findings of this study are available upon reasonable request from the authors.

Acknowledgments

This work was funded by the Korea Meteorological Administration Research and Development Program under Grant No. KMI2020-01411.

ORCID iDs

Young-Hyun Kim https://orcid.org/0000-0001-6046-3873
Joong-Bae Ahn https://orcid.org/0000-0001-6958-2801
Myoung-Seok Suh https://orcid.org/0000-0002-3827-0044
Dong-Hyun Cha https://orcid.org/0000-0001-5053-6741
Seung-Ki Min https://orcid.org/0000-0002-6749-010X

References

Ahn J B, Jo S, Suh M S, Cha D H, Lee D K, Hong S Y, Min S K, Park S C, Kang H S and Shim K M 2016 Changes of precipitation extremes over South Korea projected by the 5 RCMs under RCP scenarios *Asia-Pacific. J. Atmos. Sci.* **52** 223–36

Baldwin J W, Dessy J B, Vecchi G A and Oppenheimer M 2019 Temporally compound heat wave events and global warming: an emerging hazard *Earths Future* **7** 411–27

Chou M D 1999 Parameterization for cloud longwave scattering for use in atmospheric models *J. Clim.* **12** 159–69

Chou M D and Suarez M J 1999 *A Solar Radiation Parameterization for Atmospheric Studies*

Ciarlò J M *et al* 2021 A new spatially distributed added value index for regional climate models: the EURO-CORDEX and the CORDEX-CORE highest resolution ensembles *Clim. Dyn.* **57** 1403–24

Dong Z, Wang L, Sun Y, Hu T, Limsakul A, Singhruck P and Pimonsree S 2021 Heatwaves in southeast Asia and their changes in a warmer world *Earths Future* **9** e2021EF001992

Dosio A, Mentaschi L, Fischer E M and Wyser K 2018 Extreme heat waves under 1.5 °C and 2 °C global warming *Environ. Res. Lett.* **13** 054006

Gao M, Wang B, Yang J and Dong W 2018 Are peak summer sultry heat wave days over the Yangtze–Huaihe River basin predictable? *J. Climate* **31** 2185–96

Giorgi F, Coppola E, Raffaele F, Diro G T, Fuentes-Franco R, Giuliani G, Mamgain A, Llopar M P, Mariotti L and Torma C 2014 Changes in extremes and hydroclimatic regimes in the CREMA ensemble projections *Clim. Change* **125** 39–51

Gu H, Wang G, Yu Z and Mei R 2012 Assessing future climate changes and extreme indicatiors in east and south Asia using the RegCM4 regional climate model *Clim. Change* **144** 301–17

Im E S, Pal J S and Eltahir E A B 2017 Deadly heat waves projected in the densely populated agricultural regions of South Asia *Sci. Adv.* **3** e1603322

Im E S, Thanh N-X, Kim Y H and Ahn J-B 2019 2018 summer extreme temperatures in South Korea and their intensification under 3 °C global warming *Environ. Res. Lett.* **14** 094020

IPCC 2021 *Climate Change 2021: The Physical Science Basis Contribution of Working Group I to the Sixth Assessment Report of the Intergovernmental Panel on Climate Change* ed V Masson-Delmotte *et al* (Cambridge: Cambridge University Press)

KMA 2019 Annual report for 2018 extreme climate (Korea Meteorological Administration) pp 1–198 (available at: https://climate.go.kr/home/bbs/view.php?bname=abnormal&vcode=6232)

Kumar R and Mishra V 2019 Decline in surface urban heat island intensity in India uring heatwaves *Environ. Res. Commun.* **1** 031001

Li Z, Guo X, Yang Y, Hong Y, Wang Z and You L 2019 Heatwave trends and the population exposure over China in the 21st century as well as under 1.5 °C and 2.0 °C global warmer future scenarios *Sustainability* **11** 3318

Meehl G A and Tebaldi C 2004 More intense, more frequent, and longer lasting heat waves in the 21st century *Science* **305** 994–7

Mishra V, Mukherjee S, Kumar R and Stone D A 2017 Heat wave exposure in India in current, 1.5 °C and 2.0 °C worlds *Environ. Res. Lett.* **12** 134012

Park C, Cha D H, Kim G, Lee G, Lee D K, Suh M S, Hong S Y, Ahn J B and Min S K 2020 Evaluation of summer precipitation over far east Asia and South Korea simulated by multiple regional climate models International *J. Climatol.* **40** 2270–84

Perkins-Kirkpatrick S E and Gibson P B 2017 Changes in regional heatwave characteristics as a function of increasing global temperature *Sci. Rep.* **7** 12256

Perkins-Kirkpatrick S E and Lewis S C 2020 Increasing trends in regional heatwave *Nat. Commun.* **11** 3357

Piver W T, Ando M, Ye F and Portier C J 1999 Temperature and air pollution as risk factors for heat stroke in Tokyo, July and August 1980-1995 *Environ. Health Perspect.* **107** 911–6

Rachutorn T, Twatsupa B and Inmuong U 2019 Trends of heat-related mortality and association with weather variables in the northeast, Thailand *Environ. Asia* **12** 83–92

Rohini P, Rajeevan M and Mukhopadhay P 2019 Future projections of heat waves over India from CMIP5 models *Clim. Dyn.* **53** 975–88

Russo S, Sillmann J and Fischer E M 2015 Top ten European heatwaves since 1950 and their occurrence in the coming decades *Environ. Res. Lett.* **10** 124003

Su Q and Dong B 2019 Projected near-term changes in three types of heat waves over China under RCP4.5 *Clim. Dyn.* **53** 3751–69

Teutschbein C and Seibert J 2012 Bias correction of regional climate model simulations for hydrological climate-change impact studies: review and evaluation of different methods *J. Hydrol.* **456–457** 12–29

Thawillarp S, Thammawijaya P, Praekunnatham H and Siriruttanapruk S 2015 Situation of heat-related illness in Thailand, and the proposing of heat warning system *Outbreak Surveill Investig Rep.* **8** 15–23

Thirumalai K, DiNezio P, Okumura Y and Deser C 2017 Extreme temperatures in Southeast Aisa caused by El Nino and worsened by global warming *Nat. Commun.* **8** 15531

Torma C, Giorgi F and Coppola E 2015 Added value of regional climate modeling over areas characterized by complex terrain—precipitation over the Alps *J. Geophys. Res.* **120** 3957–72

Wang P, Hui P, Xue D and Tang J 2019 Future projection of heat waves over China under global warming within the CORDEX-EA-II project *Clim. Dyn.* **53** 957–73

WMO 2019 WMO statement on the state of the global climate in 2018 (World Meteorological Organization) pp 38

Xie W, Zhou B, Han Z and Xu Y 2021 Projected changes in heat waves over China: ensemble result from RegCM4 downscaling simulations *Int. J. Climatol.* **41** 3865–80

Yeo S, Yeh S and Lee W 2019 Two types of heat wave in Korea associated with atmospheric circulation pattern *J. Geophys. Res. Atmos.* **124** 7498–511

Yuan W *et al* 2016 Severe summer heatwave and drought strongly reduced carbon uptake in Southern China *Sci. Rep.* **6** 18813

Zhao A, Bollasina M A and Stevenson D S 2019 Strong influence of aerosol reductions on future heatwave *Geophys. Res. Lett.* **46** 4913–23